PERGAMON

Solid State Communications 119 (2001) 259–270

solid state communications

www.elsevier.com/locate/ssc

Ultrafast light-polarization dynamics in semiconductor microcavities

M.D. Martín[a], L. Viña[a,*], E.E. Mendez[b]

[a]*Departamento de Física de Materiales C-IV, Universidad Autónoma de Madrid, Cantoblanco, E-28049 Madrid, Spain*
[b]*Department of Physics and Astronomy, SUNY at Stony Brook, Stony Brook, NY 11794-3800, USA*

Abstract

We have studied the dynamics of the light emitted by a semiconductor microcavity paying special attention to the time-evolution of the degree of polarization, $\wp$, of the photoluminescence. $\wp$ depends strongly on the excitation power-density, an abrupt increase occurs when the emission becomes stimulated. Furthermore, we have found that a finite time is needed to reach the highest value of spin orientation, in contrast with the case of excitons in quantum wells where the spins are aligned almost instantly after a pulsed excitation. The faster emission dynamics of the polaritons that undergo stimulated emission, as compared with that of the polaritons with opposite spin, produces a very fast and efficient reversal of the polarization in the nonlinear regime.

PACS: 71.36.+c; 78.45.+h; 78.47.+p; 71.35.Gg

Keywords: A. Quantum wells; D. Optical properties; D. Spin dynamics; E. Time-resolved optical spectroscopies

Semiconductor electronic devices rely on the precise control of electronic charge, and in general the fact that the electrons also have a spin is ignored in practice. However, the scattering processes for electrons depend on their spin state. Recently, interest in electronic spin polarization in solid-state systems has grown fuelled by the possibility of producing efficient photoemitters with a high degree of polarization of the electron beam, creating spin memory devices and spin transistors as well as exploiting the properties of spin coherence for quantum computation. The control of the spin is very important for the development of new data storage and processing methods: a new field, known as 'spintronics', deals with the possibility of manipulation of electronic spin to read and write information through magnetism [1–8].

The properties of spin polarized carriers in bulk semiconductors, their generation, characterization and the mechanisms responsible for the spin relaxation have been profusely studied in the past [9–12]. The spin relaxation, i.e. the change in the spin state, takes place through scattering with phonons or impurities, as a consequence of the change in momentum together with the spin-orbit coupling. This process for electrons in the conduction band of bulk semiconductors appears from the mixing with finite momentum states of the valence band: Elliott–Yafet (EY) [13,14]and Dyakonov'– Perel' (DP) [15–17]mechanisms. In the case of a simultaneous existence of electrons and holes, after an optical excitation, this relaxation is due to the exchange interaction between both kinds of carriers, which is known as the Bir–Aronov–Pikus (BAP) mechanism [18]. The scattering by magnetic impurities is similar to that described by the BAP: the role of the holes is taken in this case by the localized spin in the magnetic impurity.

Experimental investigations on the spin dynamics in low-dimensional semiconductors have flourished in the last decade. In these systems, the electronic properties, compared to those of bulk semiconductors, are strongly modified by quantum size effects, and new, additional scattering mechanisms appear both for carrier transport and for the spin, due to the spatial confinement of the carriers [19,20]. Different techniques, such as time-resolved photoluminescence and 'pump and probe' spectroscopy have been used to study the spin dynamics [21–23]. In these experiments, the influence of the temperature, the doping level, the excitation power, etc. on the different spin-flip mechanisms is investigated in great detail. Their

* Corresponding author. Tel.: +34-91-397-4782; fax: +34-91-397-8579.

E-mail address: luis.vina@uam.es (L. Viña).

0038-1098/01/$ - see front matter
PII: S0038-1098(01)00115-6

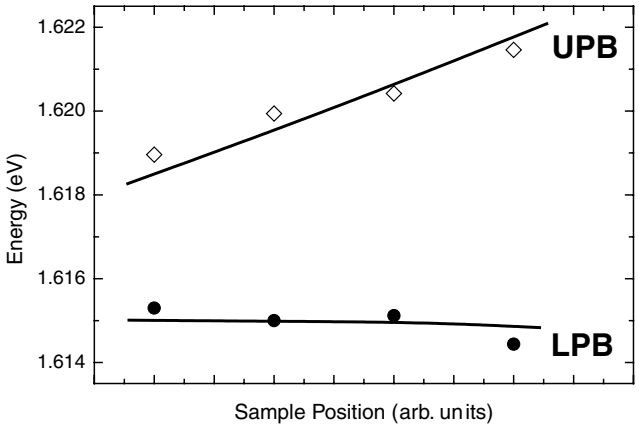

Fig. 1. LPB (●) and UPB (◇) energies as a function of the position of the excitation spot on the sample, for a time delay of 650 ps. The lines are guides to the eye.

dependence with the geometry of the quantum structures and the differences with the situation found in bulk semiconductors has been established. Many works deal with the spin processes of excitons [21,23–30], including the study of the influence of external electric fields [31]. Fewer investigations deal with the spin-flip of individuals electrons and holes in 2D systems [21,26,32,33]. Extensive theoretical studies have been also done on the spin-flip relaxation of excitons [34–37], and free carriers [19,38–40]. For a recent review see Ref. [41].

Semiconductor microcavities offer new possibilities to control the matter–radiation interaction, just by placing quantum wells (QWs) in different points of the standing wave established between the mirrors of the cavity. Since the pioneering work of Weisbuch et al. demonstrating the strong exciton-cavity coupling by the observation of the Rabi splitting [42], numerous works have dealt with the linear optical properties of the polaritons in the microcavities [43–60]. In spite of that significant changes on the spin dynamics are to be expected in semiconductor microcavities, due to the mixed photon-exciton character of the polaritons and the inefficiency of the spin-flip mechanisms on the cavity-like mode, only recently investigations on the polarization properties of VCSELs [61,62] and microcavities [63–69] have been reported. Recently, the non-linear properties of semiconductor microcavities have been the subject of intense research [65–67,70–81] due to the possibility of achieving the so-called boser effect. The saturation of the strong coupling regimen for large excitation densities has been a handicap for the study of the non-linear properties [46], however, the continuous improvement of quality of the samples has made possible the observation of polariton non-linear emission in the last 2 years [65–67,75–81].

In this paper we review the dynamics of the light emission, paying special attention to the time evolution of the polariton spin, in both linear and non-linear regimes. In particular, under high excitation, we show that the emission is highly polarized in the non-linear regime: the polarization of the radiation emitted by the coupled exciton-cavity system presents a striking behavior and its dynamics is strongly influenced by exciton-cavity detuning. These facts give experimental evidence of polaritonic stimulated emission and reveal the important role played by the spin in microcavities.

The experiments are performed in a temperature variable cryostat exciting the samples with light pulses (~2 ps, repetition rate 82 MHz) obtained from a Ti:Sapphire mode-locked laser pumped by an Ar^+-ion laser. The photoluminescence (PL) is time-resolved in a standard up-conversion spectrometer [82], using a $LiIO_3$ non-linear crystal. A double grating monochromator is used to disperse the up-converted signal. The time-resolution is limited by the pulse width and the spectral resolution is ~0.5 meV. The excitation pulses are circularly polarized by means of a $\lambda/4$ plate, and the PL is analyzed into its σ^+ and σ^-. The measurements are performed under non-resonant excitation, above the cavity stop band (1.71 eV). We present the time evolution of both the PL and its polarization degree, as a function of excitation density and exciton-cavity detuning.

The samples are grown by molecular beam epitaxy. They include dielectric mirrors separated by an $Al_{0.25}Ga_{0.75}As$ region in which three pairs of coupled GaAs QWs are placed in the antinode positions of a $3\lambda/2$ planar microcavity. The interruption of the substrate's rotation during growth originates a slight wedge in the cavity thickness, which allows tuning the cavity resonance to the transition in the QW. These microcavities have been characterized in detail under cw excitation [55].

Let us start by describing the behavior of the light emission under low excitation conditions. Fig. 1 shows the energies of the upper- and the lower-polariton branches, labeled UPB and LPB, respectively, for different positions of the excitation beam on the sample surface. These energies

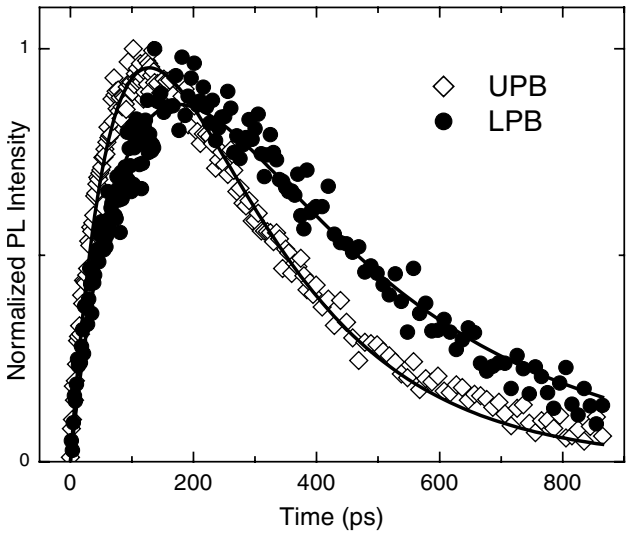

Fig. 2. Time evolution of the PL emitted by the LPB (●) and by the UPB (◇) for an excitation density of 5 W/cm^2.

are obtained from time-resolved photoluminescence spectra taken 650 ps after excitation with 5 W/cm^2. The normal mode splitting (NMS) becomes resolvable only for time delays larger than 300 ps due to the large linewidth of both polariton branches at very short times, when the polariton population is still not thermalized. The NMS varies between 3.7 and 7 meV due to the blue shift of the upper polariton branch. This fact reveals the photonic character of the UPB and the excitonic character of the LPB under these conditions. The NMS found in time-resolved experiments, which correspond to detunings between 0 and 3 meV, are comparable to those found under cw excitation, varying between 4 and 7 meV [55]. Although in this sample we have not access to negative detunings, under low excitation, we will show later that a dynamical shift of the excitonic part of the polariton, under high-excitation conditions, will allow to sample positive as well as negative detunings

The characteristic time evolution of the LPB and UPB emission is presented in Fig. 2. The rise of the PL has several contributions: the photocreated electrons and holes bind into large **K** excitons in the first tens of picoseconds [83]; these excitons scatter into LPB and UPB states and continue reducing their energy and momentum via the emission of acoustic phonons. The PL reaches its maximum when the polaritons have reached **K**~0 states. This **K**~0 population exponentially disappears via radiative recombination and escape of the polaritons out of the cavity. The time dependence, with slow rise and decay times, is similar for both polariton branches. The solid lines in Fig. 2 correspond to fits with a four-level model, which considers an initial reservoir of large **K** exciton-polaritons. The relaxation towards **K**~0 states is taken into account by the non-radiative decay of the reservoir population, characterized by τ_R^U and τ_R^L, which are the rise time of the PL emitted by the UPB and the LPB, respectively. The radiative decay from these states is described by τ_D^U and τ_D^L.

A detailed study of these characteristic rise and decay times as a function of NMS, has revealed almost no dependence on this splitting, in agreement with the results of Abram and co-workers [84] and of Sermage et al. [49] for the case of positive detunings. The characteristic times extracted from the four-level model fit are summarized in Table 1. These times have to be considered just as a first approximation to the polariton dynamics, especially in the case of the rise time, due to the simple relaxation processes considered in the model.

The analysis of the PL emitted after excitation with circularly polarized light is commonly used to study the properties of the third component of the total angular momentum J_Z, which will be called spin in the following[10,11]. A σ^+ excitation light will mainly populate the $+1$ spin level of the system. After that, a -1 spin population will appear as a result of the spin flip mechanisms, which eventually equalize both spin populations. The recombination of this -1 spin population will result in a σ^--polarized emission. The polarization degree of the PL (referred in the following simply as polarization), $\wp$, is defined as $\wp = I^+ - I^-/I^+ + I^-$, for σ^+ excitation, where $I^{+/-}$ denotes the PL intensity emitted in the σ^+ and σ^- polarization,

Table 1
Characteristic rise (τ_R) and decay (τ_D) times of the lower polariton (LPB) and upper polariton (UPB) branches extracted from a fit to a four-level model of the time evolution of the emission of each branch

	τ_R (ps)	τ_D (ps)
LPB	240 ± 20	350 ± 25
UPB	160 ± 15	185 ± 15

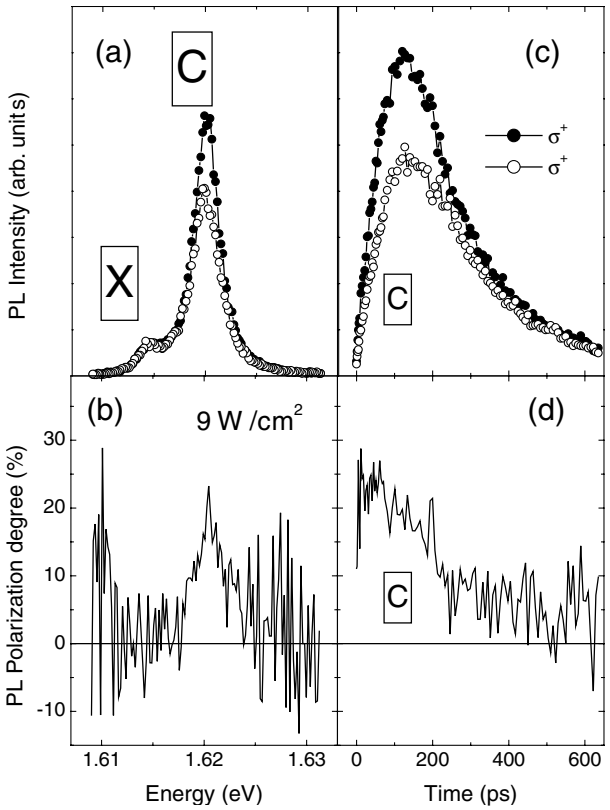

Fig. 3. (a) σ^+ (●) and σ^- (○) polarized PL spectra at 110 ps; C and X denote cavity- and exciton-like branches, respectively. (b) Polarization degree of the PL at 110 ps. (c)σ^+ (●) and σ^- (○) polarized time-evolution of the cavity-like polariton branch at ~1.62 eV. (d) Time evolution of the polarization of the cavity-like polariton branch. All the data are obtained with an excitation density of 9 W/cm^2.

respectively. In the case of the spin relaxation of cavity polaritons, their mixed radiation–matter character has to be considered. Since there is no mechanism that changes the spin of its photonic part, the spin relaxation of polaritons occurs through the spin relaxation of their excitonic component. We will show in the following that the spin dynamics of cavity polaritons is very different from that of bare excitons.

Fig. 3 summarizes the main results of the polarization- and time-resolved experiments performed with low excitation densities, 9 W/cm^2. Panel (a) shows the σ^+ (solid circles) and the σ^- (open circles) polarized components of the PL, measured at 110 ps for a NMS of 4.5 meV. The two polariton branches are resolved in the spectra and the σ^+-polarized PL intensity is larger than that of the σ^--polarized component. The different intensities of the two circularly polarized components are more evident in the cavity (C)-like polariton branch, as shown in the polarization spectrum plotted in Fig. 3(b): the polarization of the exciton (X)-like polariton branch is $<5\%$, while that of the C-like polariton branch is ~20%. The time evolutions of the σ^+- and σ^--polarized PL for the C-like polariton branch are depicted in Fig. 3(c), with the corresponding evolution of the polarization shown in Fig. 3(d): the initial polarization degree of ~20% remains nearly constant for the first 50 ps and then decays to zero as the $+1$ and -1 spin populations are equalized as a result of the spin relaxation processes. This behavior is completely different from that observed in the spin dynamics of excitons in bare QWs, where the spin relaxation processes produce an exponential decrease of the polarization to zero from its $t=0$ maximum [21]. The small initial value observed in the time evolution of the polarization is due to the non-resonant excitation conditions. In this case, electrons are promoted from $\mathbf{k}\neq 0$ states, which due to the complexity of the VB do not have a pure $\pm 3/2$ or $\pm 1/2$ spin, creating electrons with both $+1/2$ and $-1/2$ spin states in the CB. The radiative recombination of $-1/2$ spin electrons with $+3/2$ spin holes results in a σ^+-polarized emission, while the recombination of $+1/2$ spin electrons with $-3/2$ spin holes results in a σ^--polarized emission. Therefore the difference in the initial ($@t=0$) intensities of the σ^+- and the σ^--polarized PL components is directly related with the difference between the $+1/2$ and $-1/2$ spin electron populations, which is governed by the VB mixing.

The σ^+/σ^- emission intensity difference is enhanced by the increase of the excitation density, as shown in the PL

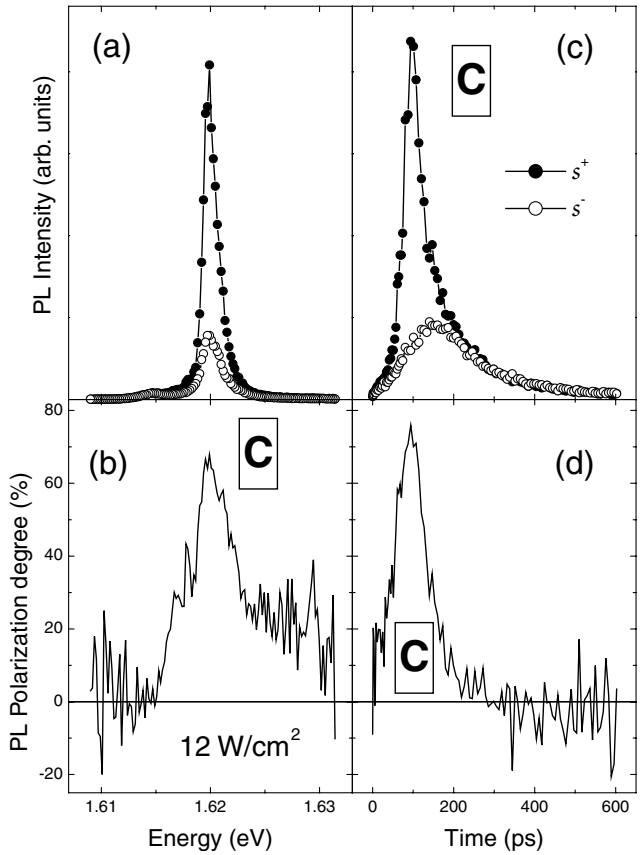

Fig. 4. (a) σ^+ (●) and σ^- (○) polarized PL spectra at 110 ps; C and X denote cavity- and exciton-like branches, respectively. (b) Polarization degree of the PL at 110 ps. (c) σ^+ (●) and σ^- (○) polarized time-evolution of the cavity-like polariton branch at ~1.62 eV. (d) Time evolution of the polarization of the cavity-like polariton branch. All the data are obtained with an excitation density of 12 W/cm^2.

spectrum depicted in Fig. 4(a), at 110 ps delay for an excitation density of 12 W/cm^2. In this case, the polarization degree of the C-like mode is ~60% (Fig. 4(b)). The recombination dynamics is progressively accelerated with increasing excitation power, a fact related with the appearance of stimulated emission, as we will show later. Fig. 4(c) shows the time evolution of the σ^+ (solid circles) and the σ^- (open circles) polarized PL of the C-like mode. The large difference in the PL intensities of the two circular components of the C-like mode turn into a large polarization degree and a conspicuous spin dynamics, as shown in Fig. 4(d): the constant polarization observed in the first 50 ps of the time evolution of $\wp$ (Fig. 3(d), 8 W/cm^2) changes into a clear polarization maximum at ~100 ps for an excitation density of 12 W/cm^2. The difference with the conventional spin dynamics of bare excitons becomes more evident in this case. The fact that a finite time is needed to reach the maximum polarization indicates that there must be a new scattering mechanism that competes with the conventional spin relaxation and which is not active in the spin dynamics of bare excitons in QWs. This new mechanism favors +1 spin polaritons while the spin relaxation processes will try to equalize both +1 and −1 spin populations. Since the strength of this new spin-aligning mechanism increases with excitation density, it is possibly related with the bosonic nature of the polaritons: the relaxation of polaritons with a given spin towards **K**~0 states is stimulated by the population of the same spin already occupying these states, as reported recently in the literature [65–67,73,75,77,85]. After reaching its maximum, the polarization degree decreases very quickly. This is due to the strong reduction of the decay time of the C-like mode as it approaches the stimulated emission regime by increasing the excitation power. The +1 spin population is emitted as σ^+-polarized PL in a fast stimulated emission process, therefore the +1/−1 spin population difference reduces very quickly, taking $\wp$ back to zero in a very short time. An additional fact corroborates the polaritonic nature of this new spin process: the maximum of polarization approaches $t = 0$ as the NMS in increased. This means that, as the excitonic component of the LPB is increased by going away from the resonance, the efficiency of the polariton stimulated scattering process decreases. The time evolution of $\wp$ continuously changes to that characteristic of bare excitons in QWs, with the

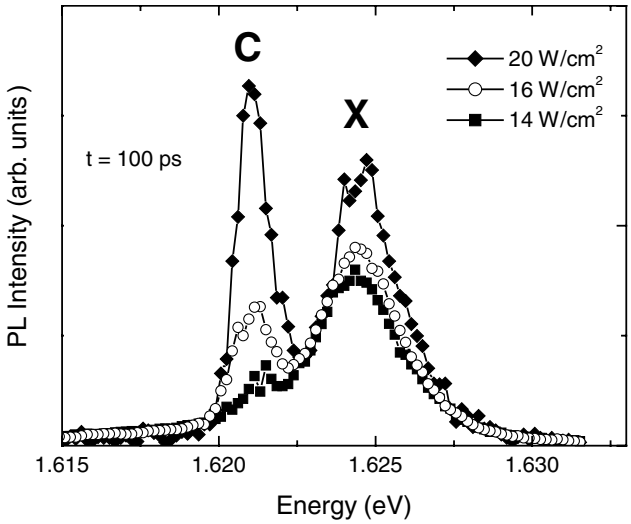

Fig. 5. PL spectra measured at 100 ps delay for different excitation densities. (■) 14 W/cm^2, (○) 16 W/cm^2 and (◆) 20 W/cm^2. X/C denote the excitonic/photonic character of the polariton branches.

maximum polarization occurring at time delays closer to $t = 0$, followed by an exponential decay.

We will concentrate now on the optical response of the microcavity under high-excitation conditions. In this regime, the results and predictions found in the literature have been the subject of new interest and controversy, due to the possibility of bleaching the polaritons under high excitation [46]. Since this plasma is characterized by a continuum energy spectrum its interaction with the cavity will be in the weak-coupling regime. In such a case the cavity will only act as a filter, allowing the transmission of light with energies similar to that of the cavity resonance. When the cavity resonance is tuned to the excitonic transition, the PL spectrum changes from a double peaked

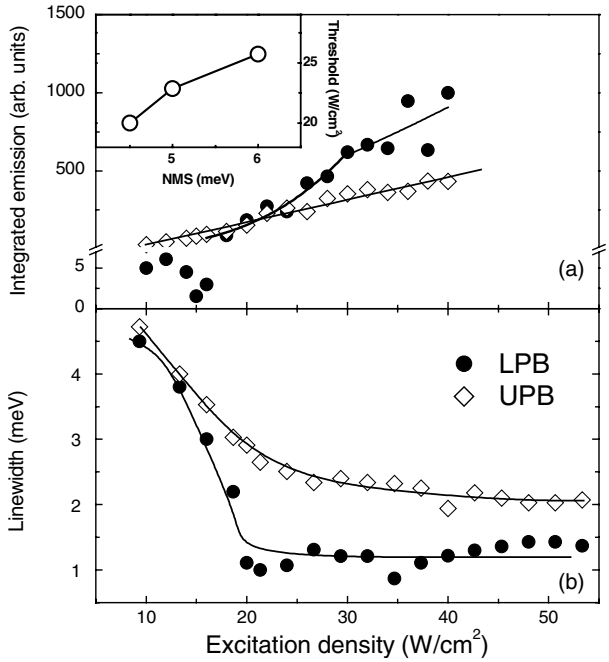

Fig. 6. (a) Integrated intensity of the LPB (●) and UPB (◇) for a time delay of 50 ps as a function of excitation power density. The inset shows the LPB excitation density threshold for different NMS. (b) Linewidth of the LPB (●) and UPB (◇) as a function of excitation density. The lines are guides to the eye.

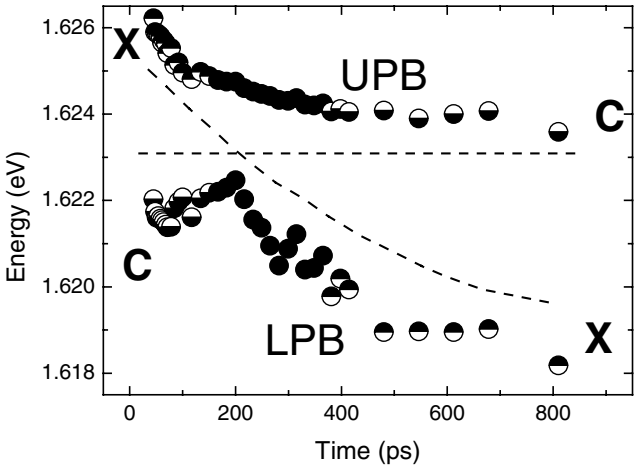

Fig. 7. Energy position of the LPB and UPB as a function of time for an I_{th} excitation density. An anticrossing is clearly observed at ~200 ps. The dashed lines are guides to the eye.

structure to single peaked [46]. However, we will show that a gradual increase of the excitation density does not bleach the polaritons in our experiments, in agreement with recent results in the literature [65–67,75–81].

Fig. 5 compiles the PL spectra at 100 ps delay for several excitation densities. The LPB becomes resolvable, as a very narrow peak (FWHM~1 meV) at 1.621 eV, at short time for excitation densities greater than 15 W/cm^2. For large excitation densities the LPB and UPB exchange their excitonic/photonic character: the UPB is exciton-like (X) and the LPB is photon-like (C). This exchange is due to the energy shift of the exciton-like polariton emission with time as will be described later. The emergence of a non-linear regime in the emission of the LPB, as the excitation power is increased, is manifested in the behavior of the integrated emission and of the linewidth of the PL shown in Fig. 6. The FWHM of the UPB decreases continuously by a factor of ~2 with increasing excitation power, while that of the LPB is reduced by a factor of ~4 with increasing excitation density and shows a marked threshold at ~20 W/cm^2 (Fig. 6(b)). Beyond this threshold its linewidth remains approximately constant at ~1 meV. The abrupt reduction of the FWHM concurs with a transition to a non-linear emission regime in the integrated emission intensity, which is shown in Fig. 6(a) for both polariton branches at a delay of 50 ps. The integrated emission of the UPB (open diamonds) shows a linear dependence with excitation power, while that of the LPB shows a more complicated behavior. For small powers ($<$18 W/cm^2) the intensity of the LPB is approximately constant, a threshold is observed at I_{th}~20 W/cm^2 (which corresponds to an injected photon density of ~2.5×10^{11} photons pulse^{-1} cm^{-2}) and a superlinear growth is obtained in the intermediate excitation power range (20–30 W/cm^2). The excitation density threshold increases slightly with increasing NMS, as depicted in the inset of Fig. 6(b). This fact is in agreement with the findings of André and co-workers, who report that the non-linear emission threshold is minimum at zero exciton-cavity detuning and that it increases when the NMS is varied, either to the positive or the negative regions [86]. For larger excitation densities ($>$30 W/cm^2) the integrated intensity shows again a linear behavior.

As mentioned above, the LPB and UPB emission energies at short times are higher than those observed at long times and there is an exchange of the excitonic/photonic character of the two polariton branches with increasing delay time. Fig. 7 depicts the emission energies of both polariton branches as a function of time for an I_{th} excitation power. At short times ($<$100 ps), the UPB has an excitonic character (X) while the LPB has a photonic character (C). As the polariton population decreases at longer times, due to its recombination, the LPB recovers its exciton-like character (X) and the UPB its photon-like character (C), as was determined by cw and long-delay time-resolved experiments performed under low excitation densities. The excitonic part of the polariton is the one that red shifts with time, while the shift of the cavity-mode is negligible as expected from its electromagnetic character. Similar shifts of excitons have been observed in bare QWs and have been attributed to exciton–exciton interaction [87–89]. A clear anticrossing of the UPB and the LPB is observed at ~200 ps. This dynamical shift of the exciton obtains negative detunings at short times, before the anticrossing takes place. The blue shift, observed at short times in our experiments, is a manifestation of many-body effects and therefore one could expect that at high exciton densities the exciton-cavity coupling would be strongly reduced. However, the observation of an anticrossing in time indicates that, in our experiments, the decrease of the exciton oscillator strength with increasing exciton population is not enough to destroy the exciton-cavity strong coupling and is a signature of the persistence of the polaritons.

The line narrowing, the excitation density threshold and

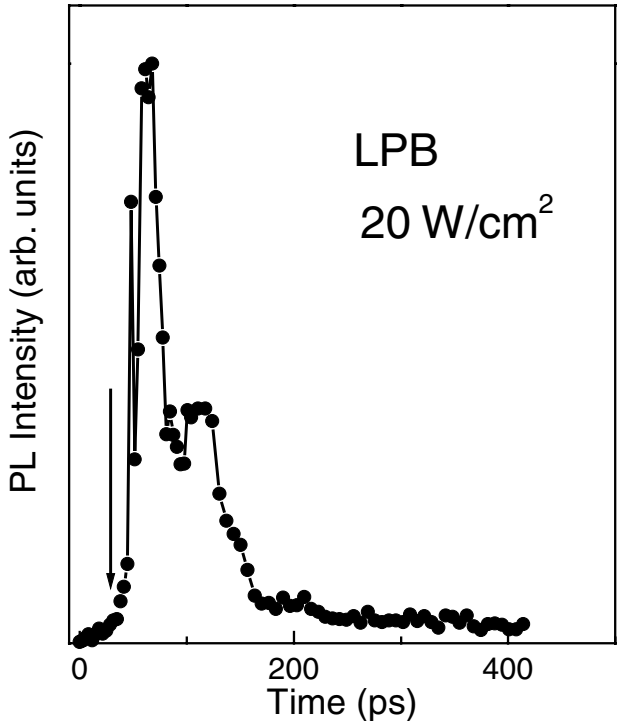

Fig. 8. Time-evolution of the PL emitted at 1.621 eV (LPB position at short times, UPB at longer times) for an excitation density of 20 W/cm^2.

the superlinear growth displayed by the emission of the LPB with increasing excitation density demonstrate its non-linear behavior. This three effects together with the anticrossing in time suggest that the PL observed above I_{th} can be attributed to stimulated emission arising from the radiative recombination of polaritons from the LPB states.

The increase of excitation power leads to several important changes also in the recombination dynamics. Fig. 8 shows the time evolution of the LPB (1.621 eV) for an excitation density of 20 W/cm^2. While the PL emission at low excitation powers is governed by a spontaneous process, which is characterized by slow rise and decay times (Fig. 2), the dynamics is accelerated and the polariton recombination process is driven by the stimulated emission at high powers. A conspicuous effect of the increase of the excitation density is the existence of a delay time for the beginning of the non-linear emission, shown by an arrow in Fig. 8. This delay corresponds to the time needed for the build up of the LPB population, and it might be related with the bottleneck in the relaxation of polaritons towards $\mathbf{K} = 0$ states [90]. The rapid rise of the PL observed beyond the threshold could be interpreted in terms of stimulated scattering, which enhances the build up of the polariton $\mathbf{K} = 0$ population. Similar delays for the beginning of the stimulated emission in semiconductor microcavities have been reported in the literature [76,91].

The time needed to reach the maximum emission (τ_{max}) and the decay time (τ_D) of the LPB are drastically reduced as the polariton system enters into the non-linear emission regime, as illustrated in Fig. 9(a) and (b), respectively for a NMS of 4.5 meV. The reduction of τ_{max} is due to a reduction of the LPB population build up time with increasing excitation density: the polariton–polariton scattering is enhanced by the increase of excitation power 65,73] leading to a faster population of $\mathbf{K} = 0$ states. τ_D decreases by approximately a factor of 5 at the threshold for stimulated emission. For excitation densities beyond the threshold the recombination dynamics is governed by the polariton stimulated emission and the decay time remains nearly constant. Both, τ_D and τ_{max} are practically independent of NMS, as they were in the case of low excitation densities [84]. A third feature in the dynamics of the light emission of the LPB shows a marked dependence on excitation power: the curvature, ζ, of the intensity vs. time, at early stages, changes from negative to positive around I_{th}. This dependence, obtained at 20 ps, is depicted in Fig. 9(c). A further increase of the excitation density above I_{th} leads to a progressive increase of the curvature. ζ increases slightly with decreasing NMS, this fact is linked with the reduction of the excitation density threshold with decreasing positive detuning, shown in the inset of Fig. 6(b).

The differences in the $+1$ and -1 spin dynamics described above for low excitation power are more evident for excitation densities above the stimulated emission threshold, revealing the non-linear origin of the processes governing both, the polariton recombination and spin

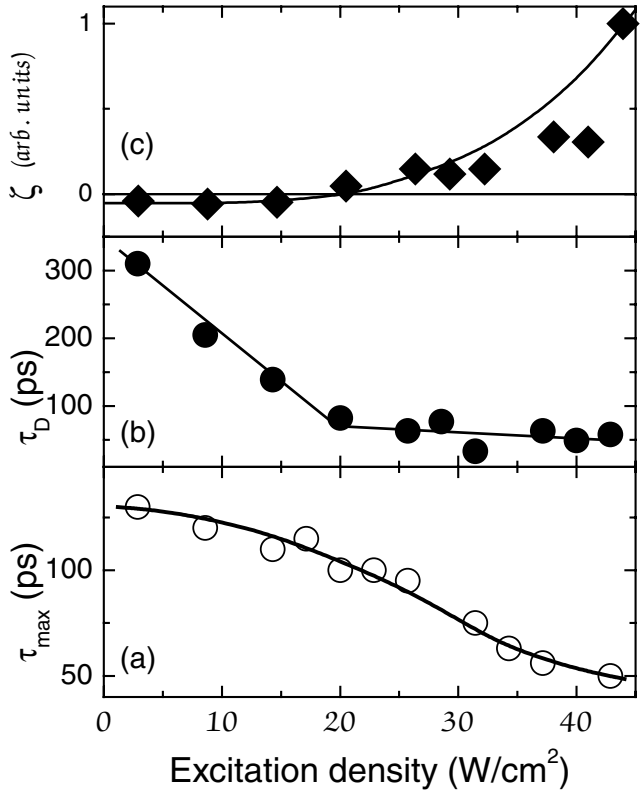

Fig. 9. (a) Time to reach the maximum emission (τ_{max}), (b) decay time (τ_D) and (c) normalized curvature (ζ) of the initial rise of the LPB, at 20 ps delay for a NMS of 4.5 meV, as a function of the excitation density. The lines are guide to the eye.

dynamics. Fig. 10 depicts the polarization-resolved PL spectra at 65 ps (panel (a)) and the time evolution of the C-like mode (panel (b)) for an excitation density $I_{th} = 20$ W/cm^2 and a NMS of 5 meV. Under such an excitation density, at short times the LPB is C-like and the UPB is X-like (see Fig. 7). It is evident in Fig. 10(a) that the intensity of the σ^+-polarized emission (solid circles) is much larger than that of the σ^--polarized one, especially in the case of the LPB. This fact reveals that the stimulated emission occurs only in the σ^+ polarization, i.e. the same as the one used for excitation.

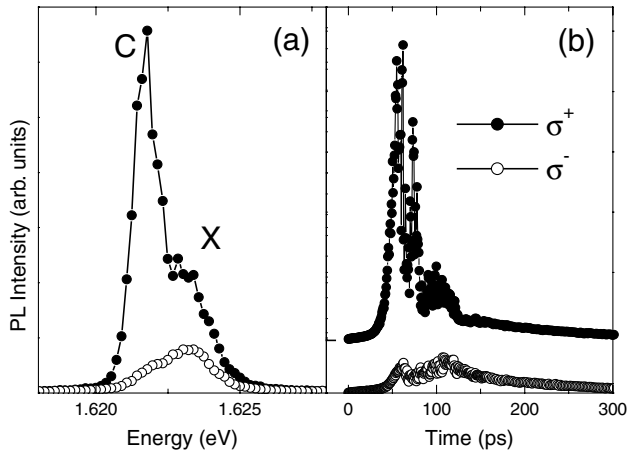

Fig. 10. (a) PL spectra at 65 ps time delay. (b) Time evolution of the cavity-like polariton branch, for σ^+ (●) and σ^- (○) polarization (the σ^+ time-evolution has been displaced for clarity). Data obtained with an I_{th} excitation density and 5 meV NMS. X/C denote the excitonic/photonic character of the polariton branches.

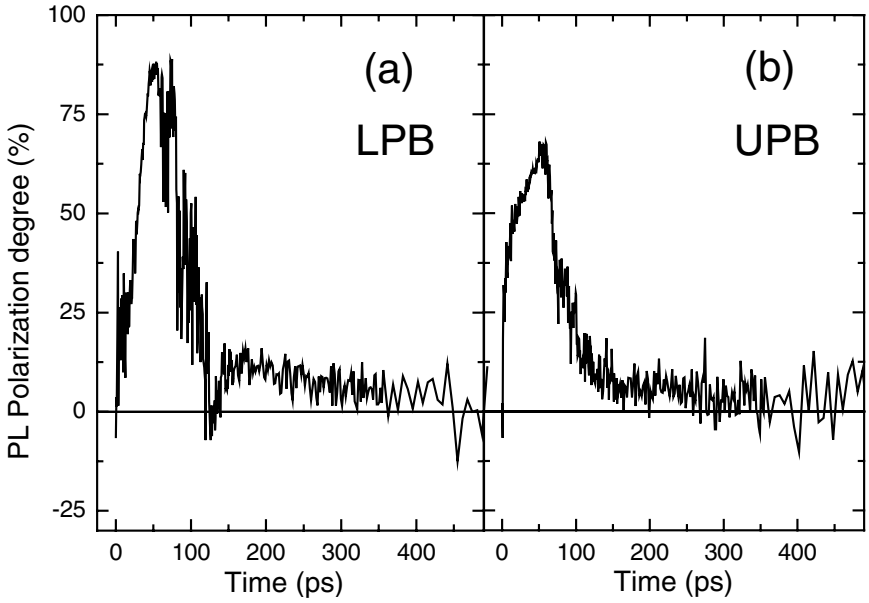

Fig. 11. Time evolution of the polarization degree of the LPB (a) and the UPB (b), under an excitation density I_{th}, for a normal mode splitting of 5 meV.

The polariton–polariton scattering is spin selective and obtains a build up of a large $+1$ spin population what leads to a very intense σ^+ stimulated emission. The time evolution traces depicted in Fig. 10(b) reveal that the σ^+ intensity, at short times, is much bigger than that of the σ^- emission due to the $+1$ spin population stimulated recombination. The rise of the σ^+-PL is very short due to the polariton–polariton stimulated scattering, reaching its maximum in ~50 ps. The stimulated scattering transfers most of the non-resonantly created polaritons to the **K**~0 LPB-states of $+1$ spin, building up a very large polarized polariton population. The decay of the σ^+-PL presents two distinct regimes. The first one, lasting up to ~100 ps, has a very fast dynamics and arises from the stimulated emission process. The second regime is characterized by a slower dynamics and arises from a spontaneous emission process. The dynamics of the -1 spin population is very different to that of the $+1$ population, not showing any evidence of stimulation and is characterized by long times. It should be mentioned that the oscillations observed in the σ^+-PL are due to the strong non-linearities and instabilities while the stimulated emission lasts.

The different $+1/-1$ spin dynamics is also evident in the polarization degree of the PL, depicted in Fig. 11 for the

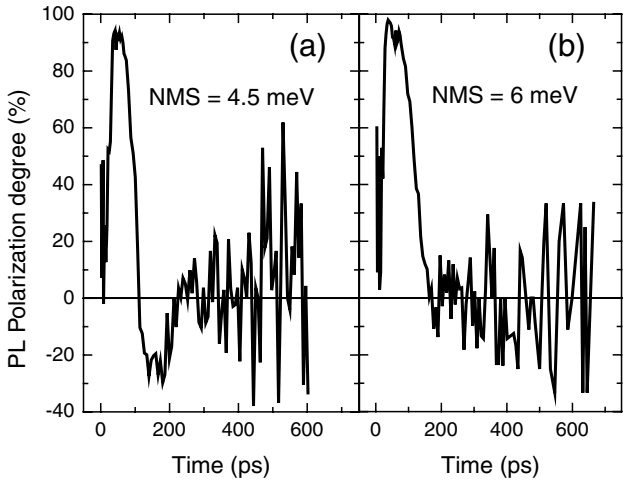

Fig. 12. Time evolution of the polarization degree of the LPB for an excitation density 1.3 I_{th} and normal mode splitting of 4.5/6 meV (a/b).

same conditions of Fig. 10. For the LPB (Fig. 11(a)), $\wp$ increases from its small initial value (~20%) as a result of the polariton final state stimulated scattering into +1 spin LPB states. This spin aligning mechanism competes with the spin relaxation processes and as a result of this competition the maximum polarization is reached at a finite time. A maximum polarization of ~90% is reached at ~50 ps, coinciding with the maximum in the σ^+-stimulated emission of the LPB. The abrupt fast decay of $\wp$ is due to the fast disappearance of the +1 polariton population due to the stimulated emission. Large polarization degrees have been observed in the LPB non-linear emission under both, cw [65] and pulsed excitation [69]. In the case of the UPB (Fig. 11(b)), the maximum of $\wp$, which also occurs at $t \neq 0$, amounts only to ~60%. This maximum at a finite time of the UPB polarization degree indicates that there is also a polariton–polariton stimulated scattering mechanism that results in a large +1 spin UPB population. However, there is no stimulated emission from the UPB due to the smaller efficiency of the scattering to UPB states compared to that to LPB states. This lower scattering efficiency is related with the smaller photonic content of the UPB at short times, which has been shown to have mainly an excitonic character.

The polarization dynamics is strongly dependent on NMS as shown in Fig. 12, which depicts the polarization degree of the LPB for a $1.3I_{th}$ excitation density and a NMS of 4.5 and 6 meV. For the case of NMS = 4.5 meV (Fig. 12(a)) a maximum polarization of ~90% is followed by a very fast decrease of $\wp$, which reaches large negative values (~ − 30%). Such a striking time evolution of the polarization degree originates mainly from the time-dependent difference of the +1 and −1 populations in the stimulated emission regime and not from spin-flip processes. At short time delays (<50 ps) the +1 spin population is much bigger than the −1 (the ratio is 95 ÷ 5 at ~50 ps). The spin selective stimulated scattering process transfers the majority of the polaritons into the +1 spin state. For intermediate delays, the large +1 population escapes the cavity through stimulated emission reducing the +1 population very quickly. The spin relaxation processes are not fast enough to compensate the fast disappearance of the +1 population so that the number of −1 spins is bigger than that of +1 and therefore the polarization becomes negative. After that, for longer time delays (>170 ps), the stimulated scattering process is not efficient any longer because the polariton population has been drastically reduced and the 'slow' spin-flip mechanisms rule the spin dynamics, making +1 and −1 populations equal, thus taking $\wp$ 'slowly' back to zero.

The spin dynamics is very different when the NMS is increased. In the case of a NMS = 6 meV (Fig. 12(b)) the maximum value of $\wp$ is again very large (>95%) but no negative polarization is observed. The polarization decay after reaching the maximum is slower than for smaller NMS. The disappearance of the +1 spin population lasts now longer due to the modification of the stimulated emission dynamics by the increase of the NMS. The spin relaxation mechanisms can now compensate the lack of +1 spin polaritons by flipping −1 spins. Both spin populations equalize bringing $\wp$ directly to zero, without reaching negative values. For excitation densities higher than $2I_{th}$ the negative dip shown in Fig. 12(a) disappears and a time evolution of the LPB polarization similar to that of larger NMS, but with faster dynamics, is obtained.

The fact that the LPB polarization changes from very large positive to negative values in just 100 ps has never been observed before in any semiconductor system, to the best of our knowledge (in the absence of magnetic fields, otherwise oscillations of the PL polarization in QW's is observed as a consequence of the Larmor precession of the spin of the holes, forming the exciton, in the field [92]). Such a fast, and with high contrast, reversal of the polarization degree could be exploited in the design of new spintronics devices, like ultrafast switches, based on the spin dynamics of microcavity-polaritons.

In summary, we have shown the existence of stimulated processes for the lower polariton branch in microcavities, revealed by drastic changes in the photoluminescence and its time evolution as a function of excitation density. Polarization-resolved measurements show that the stimulation is spin selective and leads to very high values of the polarization. The polariton-spin dynamics is very different to that of bare excitons: the spins are realigned giving rise to a polarization maximum at finite times. This dynamics is strongly influenced by the normal mode splitting, obtaining a sharp swap from very large positive to negative values of $\wp$ for small exciton-cavity detuning.

Acknowledgements

This research has been partially supported by the Fundación Ramón Areces, the Spanish DGICYT under contract PB96-0085, and US Army Research Office. We are thankful to Dr I. W. Tao and R. Ruf for growing the samples.

References

[1] G.A. Prinz, Science 282 (1998) 1660.
[2] R. Fiederling, et al., Nature 402 (1999) 787.
[3] Y. Ohno, et al., Nature 402 (1999) 790.
[4] S. Gardelis, et al., Phys. Rev. B 60 (1999) 7764.
[5] R.D.R. Bhat, J.E. Sipe, Phys. Rev. Lett. 85 (2000) 5432.
[6] I. Malajovich, et al., Phys. Rev. Lett. 84 (2000) 1015.
[7] H. Ohno, Science 291 (2001) 840.
[8] Y. Matsumoto, et al., Science 291 (2001) 854.
[9] G.E. Pikus, E.L. Ivchenko, in: E.I. Rashba, M.D. Sturge (Eds.), Excitons, North-Holland, Amsterdam, 1982, p. 205.
[10] M.I. D'yakonov, V.I. Perel', in: F. Maier, B.P. Zakharchenya (Eds.), Optical Orientation, Elsevier Science Publishers, Amsterdam, 1984, p. 12.

[11] G.E. Pikus, A.N. Titkov, in: F. Maier, B.P. Zakharchenya (Eds.), Optical Orientation, Elsevier Science Publishers, Amsterdam, 1984, p. 73.
[12] E.J. Johnson, R.J. Seymour, R.R. Alfano, in: R.R. Alfano (Ed.), Semiconductors Probed by Ultrafast Laser Spectroscopy, vol. 2, Academic, New York, 1984, p. 200.
[13] R.J. Elliot, Phys. Rev. 96 (1954) 266.
[14] Y. Yafet, in: F. Seitz, D. Turnbull (Eds.), Solid State Physics, Academic, New York, 1963, p. 1.
[15] M.I. D'yakonov, V.I. Perel', Sov. Phys. JETP 33 (1971) 1053.
[16] M.I. D'yakonov, V.I. Perel', Sov. Phys.-Solid State 13 (1972) 3023.
[17] V.D. Dymnikov, M.I. D'yakonov, V.I. Perel', Sov. Phys. JETP 44 (1976) 1252.
[18] G.L. Bir, A.G. Aronov, G.E. Pikus, Sov. Phys. JETP 42 (1976) 705.
[19] M.I. D'yakonov, V.Yu. Kachorovskii, Sov. Phys. Semicond. 20 (1986) 110.
[20] L.J. Sham, J. Phys.: Cond. Matter 5 (1993) A51.
[21] T.C. Damen, et al., Phys. Rev. Lett. 67 (1991) 3432.
[22] M. Kohl, M.R. Freeman, D.D. Awshalom, J.M. Hong, Phys. Rev. B 44 (1991) 5923.
[23] L. Muñoz, E. Perez, L. Viña, K. Ploog, Phys. Rev. B 51 (1995) 4247.
[24] A. Takeuchi, Y. Nishikawa, O. Wada, Appl. Phys. Lett. 68 (1996) 797.
[25] M.R. Freeman, et al., Phys. Rev. Lett. 64 (1990) 2430.
[26] P. Roussignol, et al., Phys. Rev. B 46 (1992) 7292.
[27] A. Vinattieri, et al., Solid State Commun. 88 (1993) 189.
[28] T. Amand, et al., Phys. Rev. B 55 (1997) 9880.
[29] R.S. Britton, et al., Appl. Phys. Lett. 73 (1998) 2140.
[30] A. Malinowski, et al., Phys. Rev. B 62 (2000) 13034.
[31] A. Vinattieri, et al., Appl. Phys. Lett. 63 (1993) 3164.
[32] E.L. Ivchenko, et al., JETP Lett. 47 (1988) 486.
[33] J. Wagner, et al., Phys. Rev. B 47 (1993) 4786.
[34] L.J. Sham, J. Phys. (Paris), Colloq. 48 (1987) C5–381.
[35] T. Uenoyama, L.J. Sham, Phys. Rev. B 42 (1990) 7114.
[36] M.Z. Maialle, E.A. de Andrade e Silva, J. Sham, Phys. Rev. B 47 (1993) 15776.
[37] E.A. de Andrade e Silva, G.C.L. Rocca, Phys. Rev. B 56 (1997) 9259.
[38] G. Bastard, R. Ferreira, Surface Sci. 267 (1992) 335.
[39] R. Ferreira, G. Bastard, Solid State Electr. 37 (1994) 851.
[40] M.Z. Maialle, M.H. Degani, Phys. Rev. B 55 (1997) 13771.
[41] L. Viña, J. Phys.: Cond. Matt. 11 (1999) 5929 and references therein.
[42] C. Weisbuch, M. Nishioka, A. Ishikawa, Y. Arakawa, Phys. Rev. Lett. 69 (1992) 3314.
[43] R. Houdré, et al., Phys. Rev. Lett. 73 (1994) 2043.
[44] T.B. Norris, et al., Phys. Rev. B 50 (1994) 14663.
[45] R. Houdré, et al., Phys. Rev. B 49 (1994) 16761.
[46] R. Houdré, et al., Phys. Rev. B 52 (1995) 7810.
[47] T.A. Fisher, et al., Phys. Rev. B 51 (1995) 2600.
[48] J. Tignon, et al., Phys. Rev. Lett. 74 (1995) 3967.
[49] B. Sermage, et al., Phys. Rev. B 53 (1996) 16516.
[50] T. Tanaka, et al., Appl. Phys. Lett. 69 (1996) 887.
[51] J. Bloch, J.Y. Marzin, Phys. Rev. B 53 (1997) 2103.
[52] J. Tignon, et al., Phys. Rev. B 56 (1997) 4068.
[53] A. Armitage, et al., Phys. Rev. B 55 (1997) 16395.
[54] J.J. Baumberg, A. Armitage, M.S. Skolnick, J.S. Roberts, Phys. Rev. Lett. 81 (1998) 661.
[55] I.W. Tao, et al., Physica E 2 (1998) 685.
[56] M.S. Skolnick et al., in: D. Gershoni (Ed.), Proceedings of the 24th International Conference on the Physics of Semiconductors, World Scientific Singapore, 1999, p. 25.
[57] M. Opher-Lipson, et al., Phys. Rev. B 59 (1999) 10261.
[58] R. Harel, A. Ron, E. Linder, L.N. Pfeiffer, Phys. Rev. B 60 (1999) 11550.
[59] G. Martinez, R. Aguilar, P.H. Hernández, G. Cocoletzi, Phys. Rev. B 62 (2000) 6916.
[60] M. Müller, J. Bleuse, R. André, Phys. Rev. B 62 (2000) 16886.
[61] H. Ando, T. Sogawa, H. Gotoh, Appl. Phys. Lett. 73 (1998) 566.
[62] A. Gahl, S. Balle, M. San Miguel, IEEE J. Quantum Elect. 35 (1999) 342.
[63] S. Hallstein, et al., Phys. Rev. B 56 (1997) R7076.
[64] M.D. Martin et al., in: D. Gershoni (Ed.), Proceedings of the 24th International Conference on the Physics of Semiconductors, World Scientific Singapore, 1999, CD-ROM: 0285.pdf.
[65] A.I. Tartakowskii, et al., Phys. Rev. B 60 (1999) R11293.
[66] M.D. Martín, L. Viña, J.K. Son, E.E. Mendez, Solid State Commun. 117 (2001) 267.
[67] M.D. Martin et al., in: T. Ando (Ed.), Proceedings of the 25th International Conference on the Physics of Semiconductors, Osaka, Japan, September 2000, Springer, New York, 2001.
[68] X. Marie, et al., Phys. Rev. B 59 (1999) R2494.
[69] P. Renucci et al., in: T. Ando (Ed.), Proceedings of the 25th International Conference on the Physics of Semiconductors, Osaka, Japan, September 2000, Springer, New York, 2001.
[70] S. Pau, et al., Phys. Rev. A 54 (1996) R1789.
[71] X. Fan, H. Wang, H.Q. Hou, B.E. Hammons, Phys. Rev. B 56 (1997) 15256.
[72] F. Quochi, et al., Phys. Rev. B 59 (1999) R15594.
[73] T. Baars, et al., Phys. Rev. B 61 (2000) R2409.
[74] F. Quochi, et al., Phys. Rev. Lett. 80 (1998) 4733.
[75] L.S. Dang, et al., Phys. Rev. Lett. 81 (1998) 3920.
[76] J. Bleuse, J. Crystal, et al., Growth 184–185 (1998) 750.
[77] P. Senellart, J. Bloch, Phys. Rev. Lett. 82 (1999) 1233.
[78] P.G. Savvidis, et al., Phys. Rev. Lett. 84 (2000) 1547.
[79] G. Dasbach, et al., Phys, Rev. B 62 (2000) 13076.
[80] J.J. Baumberg, et al., Phys. Rev. B 62 (2000) R16247.
[81] P. Senellart, J. Bloch, B. Sermage, J.Y. Marzin, Phys. Rev. B 62 (2000) R12263.
[82] J. Shah, IEEE J. Quantum Electron. 24 (1988) 276.
[83] J. Shah, Ultrafast Spectroscopy of Semiconductors and Semiconductor Heterostructures, Springer, Berlin, 1996.
[84] I. Abram, et al., in: J. Rarity, C. Weisbuch, et al. (Eds.), Microcavities and Photonic Bandgaps: Physics and Applications, NATO ASI Series E, vol. 324, Kluwer Academic Publishers, Dordrecht, 1996, p. 69.
[85] F. Tassone, Y. Yamamoto, Phys. Rev. B 59 (1999) 10830.
[86] R. André et al., in: D. Gershoni (Ed.), Proceedings of the 24th International Conference on the Physics of Semiconductors, World Scientific Singapore, 1999, CD-ROM: 1089.pdf.
[87] N. Peyghambarian, et al., Phys. Rev. Lett. 53 (1984) 24331.
[88] S. Schmitt-Rink, D.S. Chemla, D.A.B. Miller, Phys. Rev. B 32 (1985) 6601.
[89] D. Hulin, et al., Phys. Rev. B 33 (1986) 4389.
[90] F. Tassone, et al., Phys. Rev. B 56 (1997) 7554.
[91] V. Mizeikis et al., in: T. Ando (Ed.), Proceedings of the 25th International Conference on the Physics of Semiconductors, Osaka, Japan, September 2000, Springer, New York, 2001.
[92] X. Marie, et al., Phys. Rev. B 60 (1999) 5811.